

Supporting Information

**Uniform Synthesis of Palladium Species Confined in Small-pore zeolite via
Full Ion-exchange Investigated by Cryogenic Electron Microscopy**

Yongwoo Kim[†], Jongbaek Sung[†], Sungsu Kang, Jaeha Lee, Min-Ho Kang, Sungha Hwang,
Hayoung Park, Joodeok Kim, Younhwa Kim, Eunwon Lee, Gyeong-Su Park, Do Heui Kim*
Jungwon Park*

Supporting figures

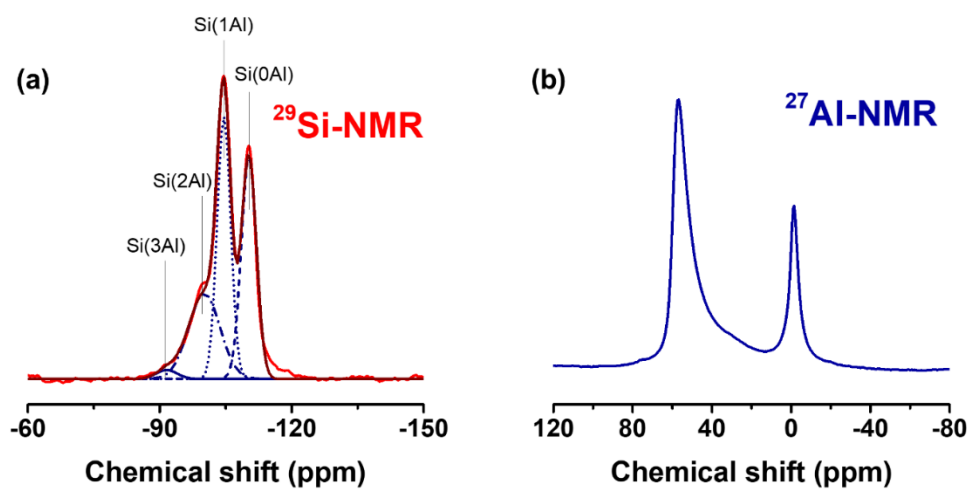


Figure S1. (a) Si-MAS-NMR with deconvolution and (b) Al-MAS-NMR spectra of $\text{NH}_4\text{-SSZ-13}$. The Si-to-Al ratio was measured from Si-MAS-NMR.

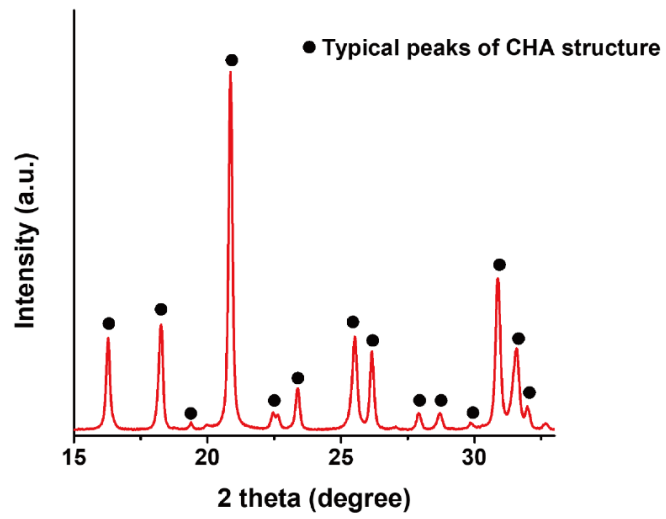


Figure S2. XRD pattern of the NH₄-SSZ-13.

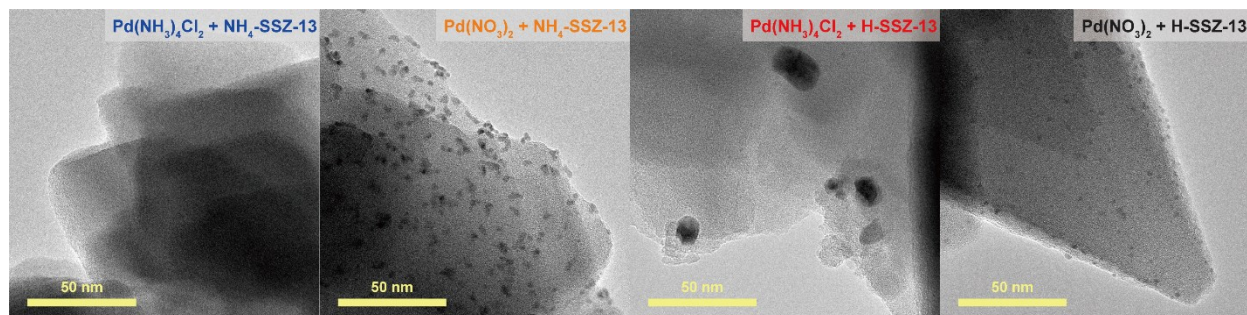


Figure S3. Magnified TEM images of the fresh Pd-exchanged SSZ-13 samples prepared using different combinations of precursors and zeolite-forms, before the calcination step.

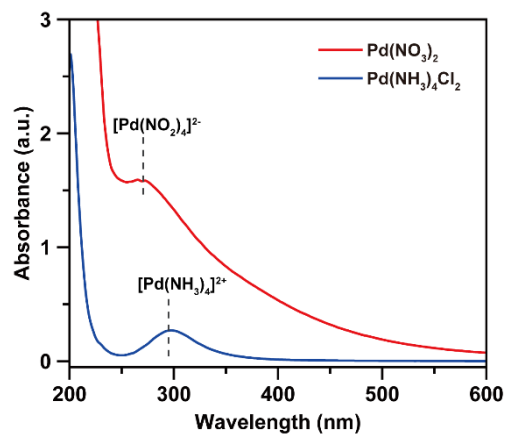


Figure S4. UV-vis spectra of $\text{Pd}(\text{NO}_3)_2$ and $\text{Pd}(\text{NH}_3)_4\text{Cl}_2$ solutions.

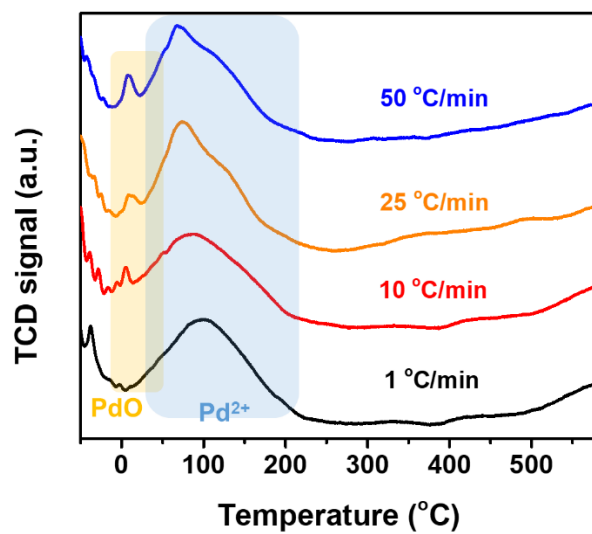


Figure S5. Cryo-H₂-TPR profiles of the Pd-exchanged SSZ-13 samples prepared with Pd(NH₃)₄Cl₂ and NH₄-SSZ-13 with different ramping rates for calcination.

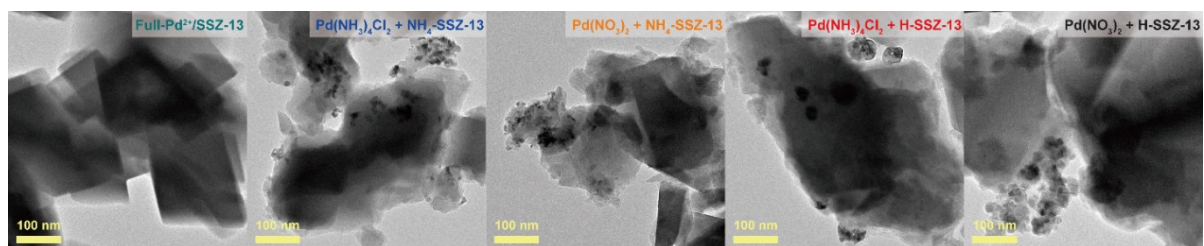


Figure S6. TEM images of the Pd-exchanged SSZ-13 samples prepared with different combinations of Pd precursors and zeolite-forms, after the calcination step. The sample with full ion-exchange efficiency (Full-Pd²⁺/SSZ-13) was calcined with the ramping rate of 1 °C/min, while the other samples are calcined with the ramping rate of 10 °C/min.

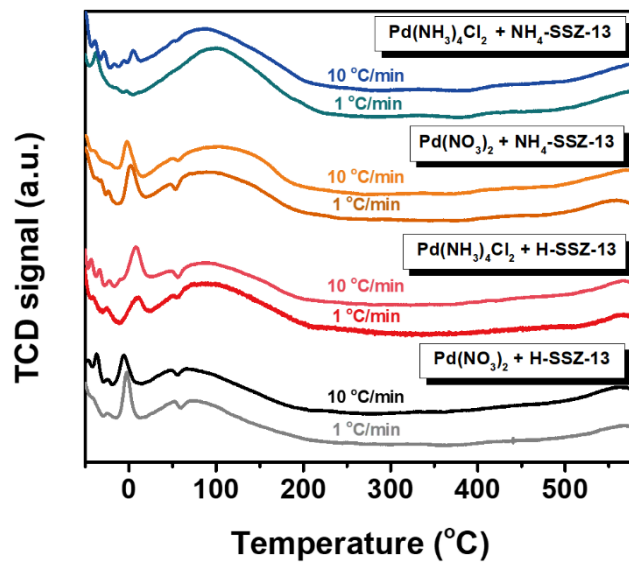


Figure S7. Cryo-H₂-TPR profiles of the Pd-exchanged SSZ-13 samples prepared using different combinations of precursors, zeolite-forms, and ramping rates (i.e. 1 °C/min and 10 °C/min) for calcination. The absence of PdO peak at approximately 0 °C was only shown in the sample prepared using Pd(NH₃)₄Cl₂ and NH₄-SSZ-13 with the ramping rate of 1 °C/min for calcination.

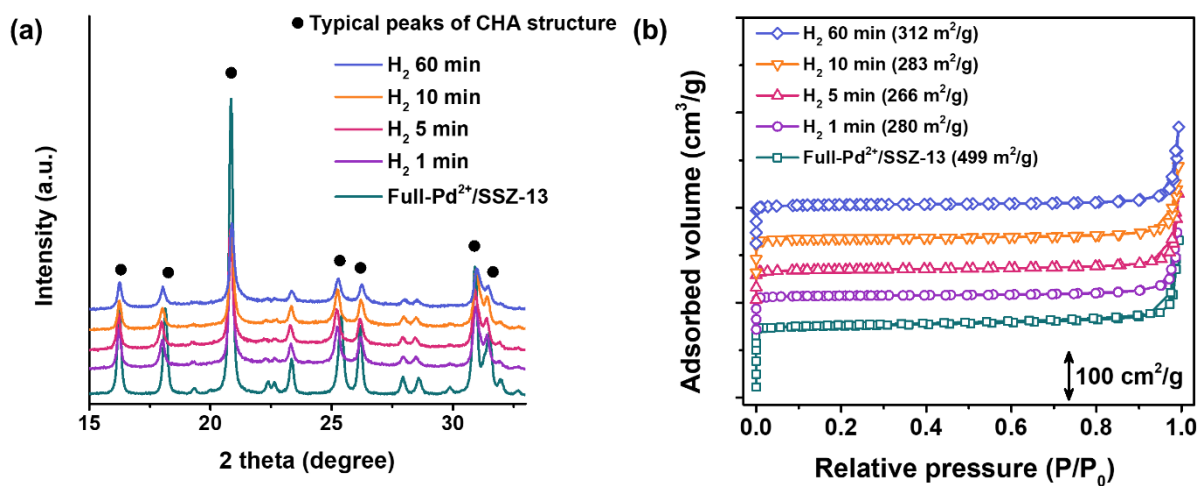


Figure S8. (a) XRD patterns and (b) N₂ adsorption-desorption profiles of the Full-Pd²⁺/SSZ-13 and the thermal-treated Pd/SSZ-13 catalysts with different H₂ treatment times.

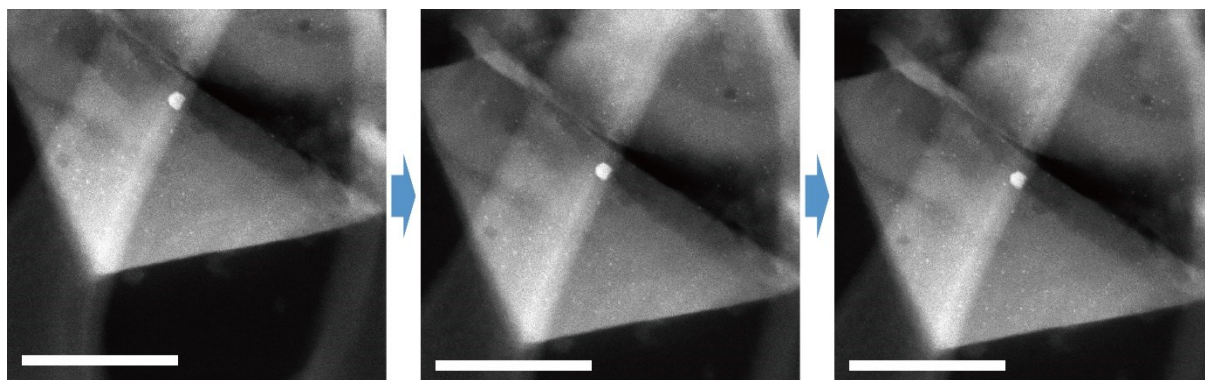


Figure S9. Serial Cryo-STEM images of the ultramicrotomed thermal-treated Pd/SSZ-13 catalyst with H₂ treatment time of 5 min. The negligible difference in the size of internal Pd species and the structure of zeolite at serial images indicate that the electron-beam induced damage is significantly suppressed. Scale bars are 100 nm.

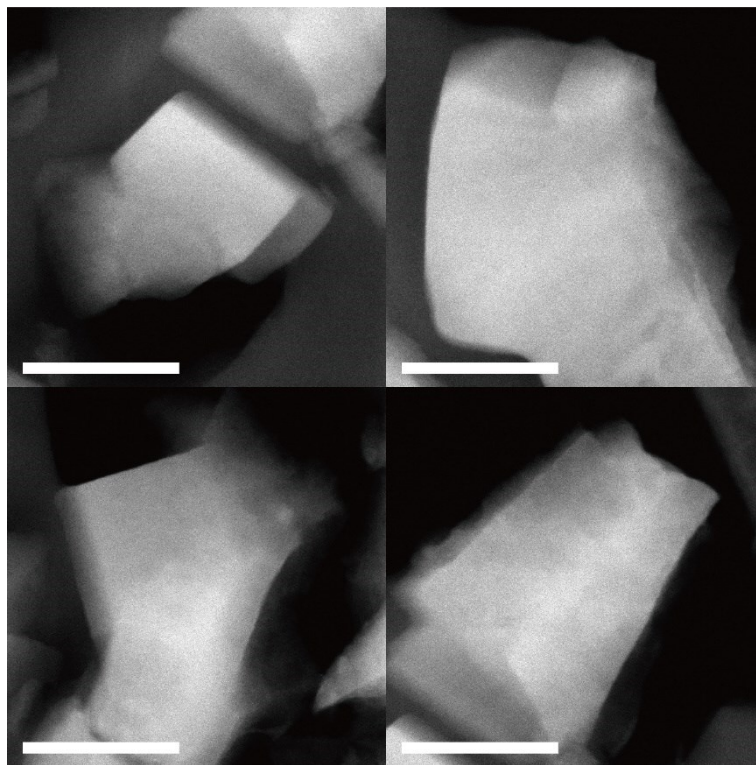


Figure S10. Cryo-STEM images of the ultramicrotomed Full-Pd²⁺/SSZ-13. Owing to the full ion-exchange and the successful minimization of the electron-beam induced damage, the Pd species are unobservable in cryo-STEM images of the ultramicrotomed Full-Pd²⁺/SSZ-13. Scale bars are 100 nm.

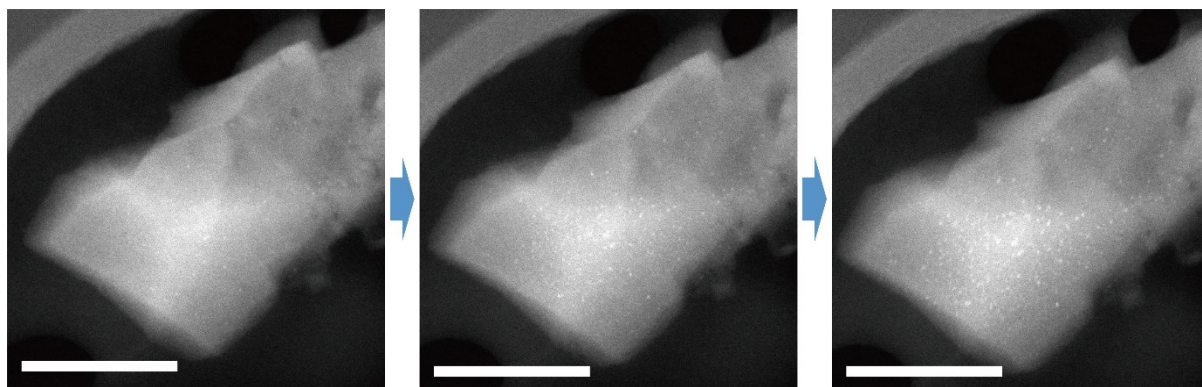


Figure S11. Serial STEM images of ultramicrotomed Full-Pd²⁺/SSZ-13 obtained under conventional STEM mode, starting from the initial time period of imaging. Compared to the cryo-STEM images in Figure S9 and S10, the agglomeration of isolated Pd²⁺ ions was observed even at the early stage of imaging, and becomes severe after multiple scanings. Scale bars are 100 nm.

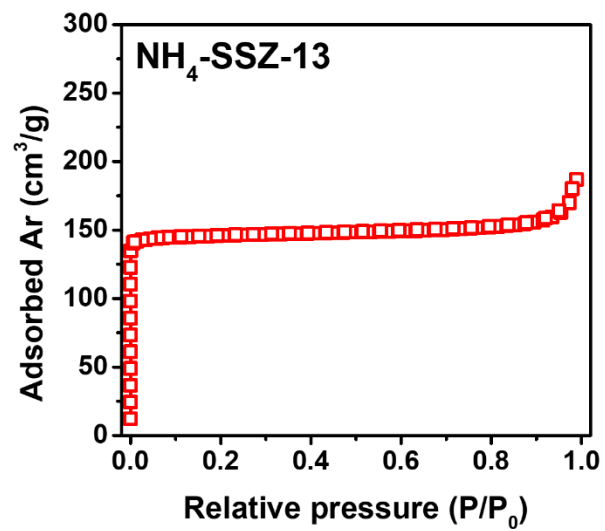


Figure S12. Ar adsorption-desorption isotherm of NH₄-SSZ-13

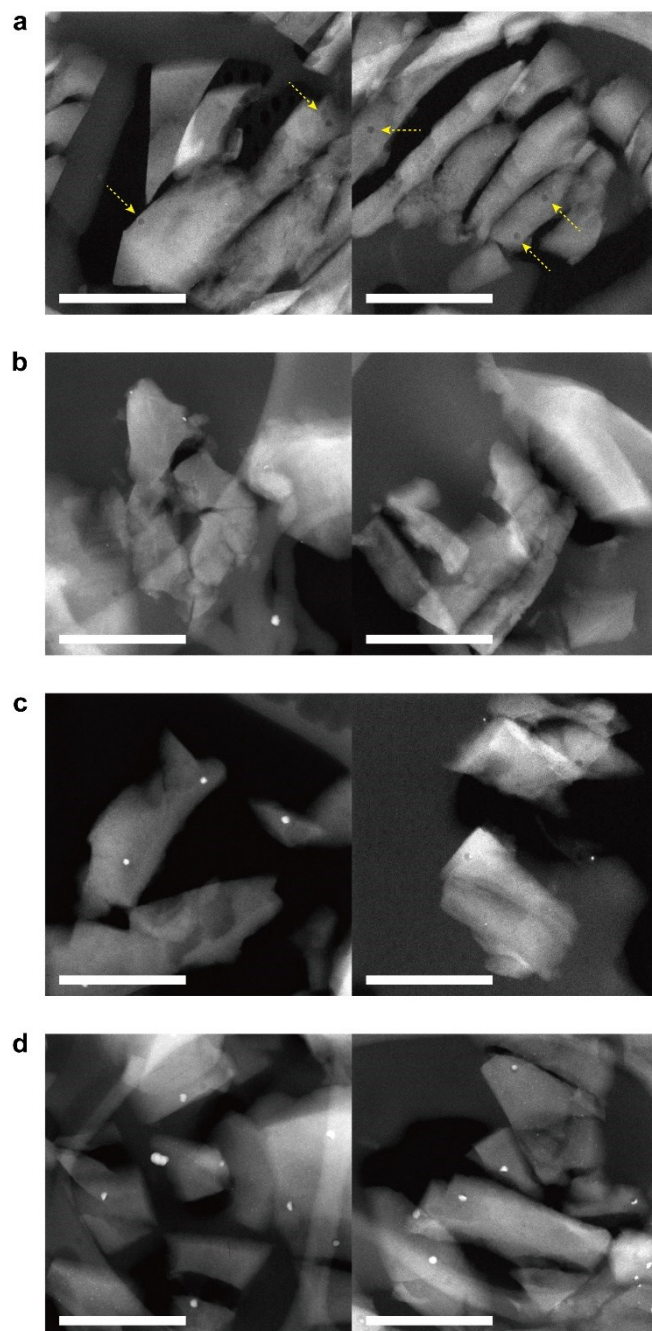


Figure S13. Low-magnification Cryo-STEM images of the ultramicrotomed thermal-treated Pd/SSZ-13 catalyst with H₂ treatment time of (a) 1 min, (b) 5 min, (c) 10 min, and (d) 60 min. The presence of internal void sites is indicated with yellow arrows in (a). The development of Pd species at the internal void sites according to the H₂ treatment time is observed. Scale bars are 200 nm.

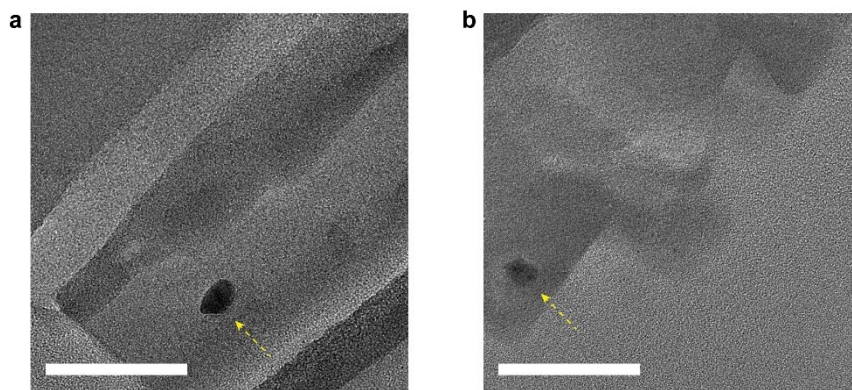


Figure S14. Low-magnification Cs-corrected TEM images of Pd species generated in the internal void site of the ultramicrotomed thermal-treated Pd/SSZ-13 with H₂ treatment time of 60 min. The high resolution TEM image and the structural information of each Pd species in (a) and (b) are illustrated in Figure 4b and 4c, respectively. Scale bars are 50 nm.

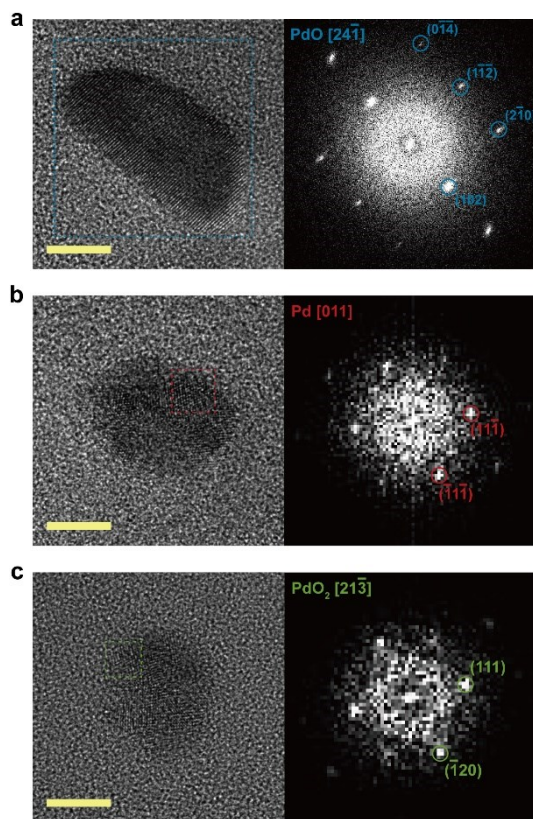


Figure S15. Cs-corrected TEM images and selected-area fast Fourier transform (FFT) patterns of Pd species developed in the internal void site of the ultramicrotomed thermal-treated Pd/SSZ-13 with H₂ treatment time of 60 min. Along with PdO, Pd and PdO₂ phases are also designated. Scale bars are 5 nm.

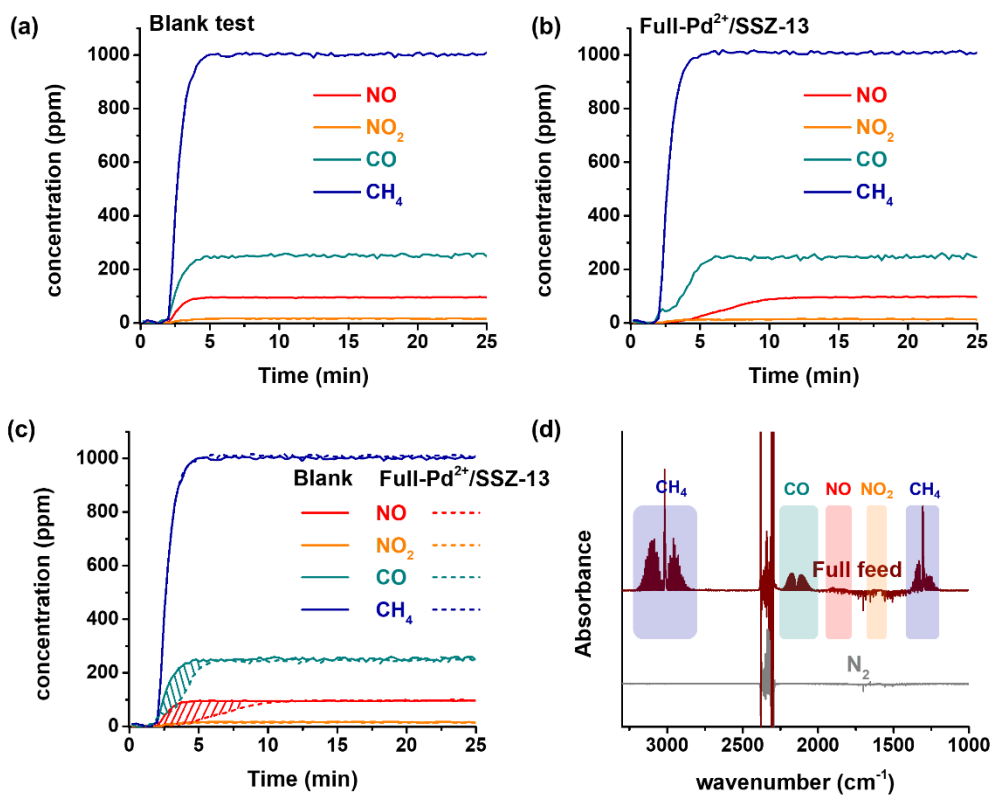


Figure S16. The changes in the outlet concentration of NO, NO₂, CO, and CH₄ analyzed by FT-IR series methods (a) without any catalysts, (b) with Full-Pd²⁺/SSZ-13 catalyst, and (c) their combined data showing the difference (the colored areas originated from the adsorption of reactants); (d) IR spectra obtained by IR series method under N₂ condition and full feed condition.

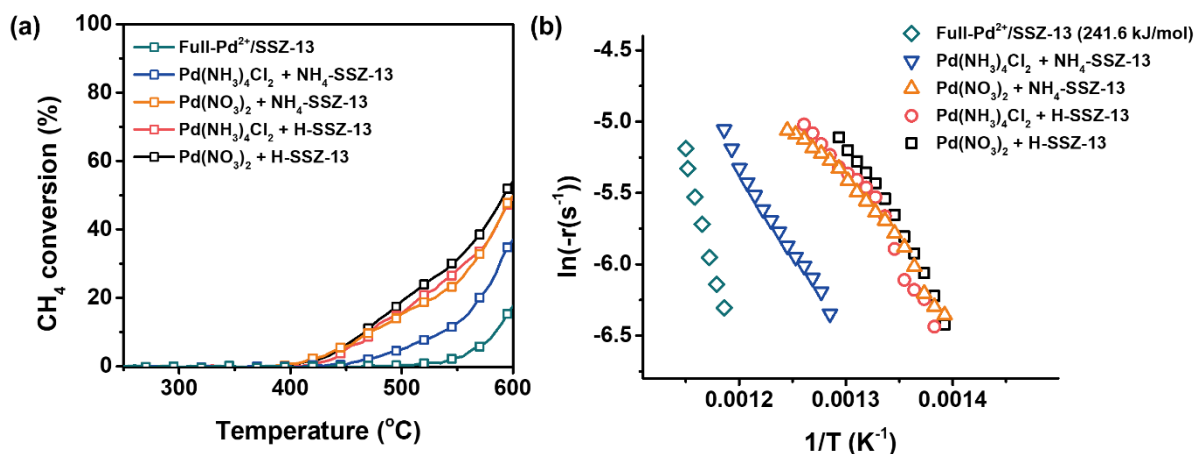


Figure S17. (a) CH₄ combustion light-off curves and (b) Arrhenius plots of the Full-Pd²⁺/SSZ-13 and other Pd/SSZ-13 catalysts after air calcination of 500 °C for 2 h and without any treatment. As PdO is the active phase for CH₄ combustion, the catalytic activities were increased with the higher portion of PdO which was observed in H₂-TPR (Figure 1b). However, the activation energies for most catalysts could not be measured based on the Arrhenius plots. Since both PdO and isolated Pd²⁺ ions were present in those catalysts, the Arrhenius relationship was affected by the activation of CH₄ oxidation over both PdO and isolated Pd²⁺ ions, resulting in the non-linear correlation of the Arrhenius plot.

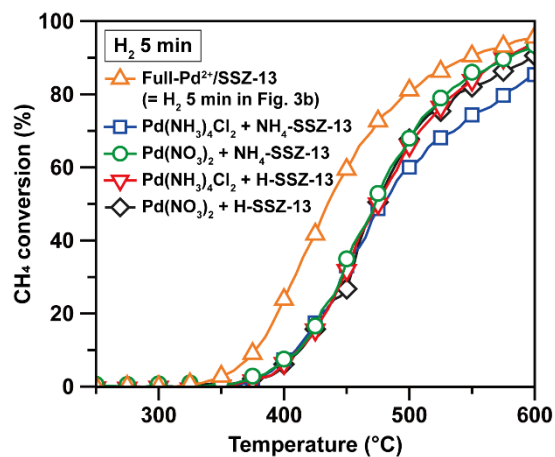


Figure S18. CH₄ combustion light-off curves of the thermal-treated Pd/SSZ-13 catalysts with same H₂ treatment time of 5 min, but prepared using different combinations of the Pd precursors, zeolite-forms, and ramping rate.

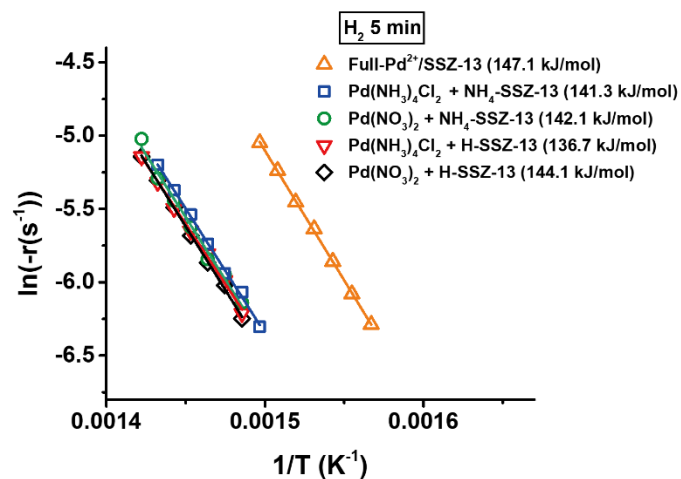


Figure S19. Arrhenius plot of CH₄ combustion over the thermal-treated Pd/SSZ-13 catalysts prepared from different combination of Pd precursors and zeolite-forms with 5 min H₂ treatment.

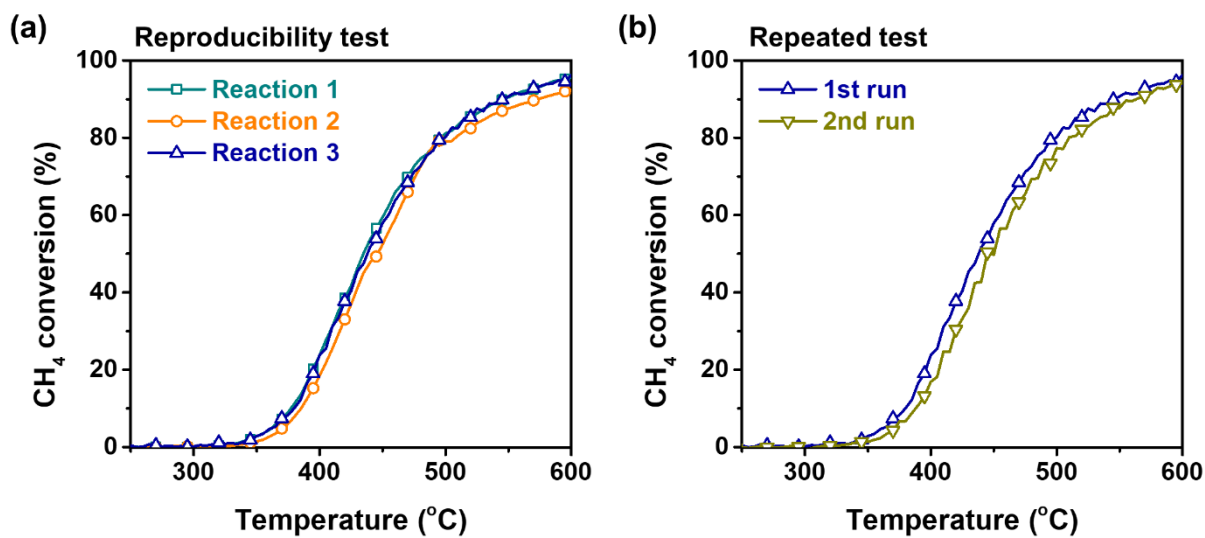


Figure S20. (a) Reproducibility test and (b) repeated test for CH₄ combustion over the thermal-treated Full-Pd²⁺/SSZ-13 catalyst with H₂ treatment for 5 min. The reproducibility test was performed over the samples prepared in different batches, whereas the repeated test was carried out by successive reaction tests over the same sample.

Supporting tables

Table S1. Textual properties of SSZ-13 obtained from Ar-adsorption isotherm.

Sample	BET surface area (m ² /g)	Average pore diameter (nm)	Micropore area (m ² /g)	Micropore volume (cm ³ /g)
NH ₄ -SSZ-13	532	1.8	520	0.182

Table S2. Compositional properties of Pd-exchanged SSZ-13 samples.

Sample	Si/Al ratio ^a	H ⁺ /Al (before Pd ²⁺ exchange) ^b	Pd content (wt%) ^c	Pd/Al ^b	Molecular formula
Pd(NO ₃) ₂ 2H ₂ O + H-SSZ-13			0.86	0.028	
Pd(NH ₃) ₄ Cl ₂ H ₂ O + H-SSZ-13			0.88	0.029	
Pd(NO ₃) ₂ 2H ₂ O + NH ₄ -SSZ-13	4.5	0.85	0.91	0.030	Pd _{0.0005} Si _{0.81} Al _{0.18} O ₂
Pd(NH ₃) ₄ Cl ₂ H ₂ O + NH ₄ -SSZ-13			0.94	0.029	
Full-Pd ²⁺ /SSZ-13			0.91	0.030	

^a Determined by ²⁹Si-MAS-NMR.

^b Determined by ICP-AES after the ion-exchange of NH₄-SSZ-13 with NaNO₃.

^c Determined by ICP-AES.

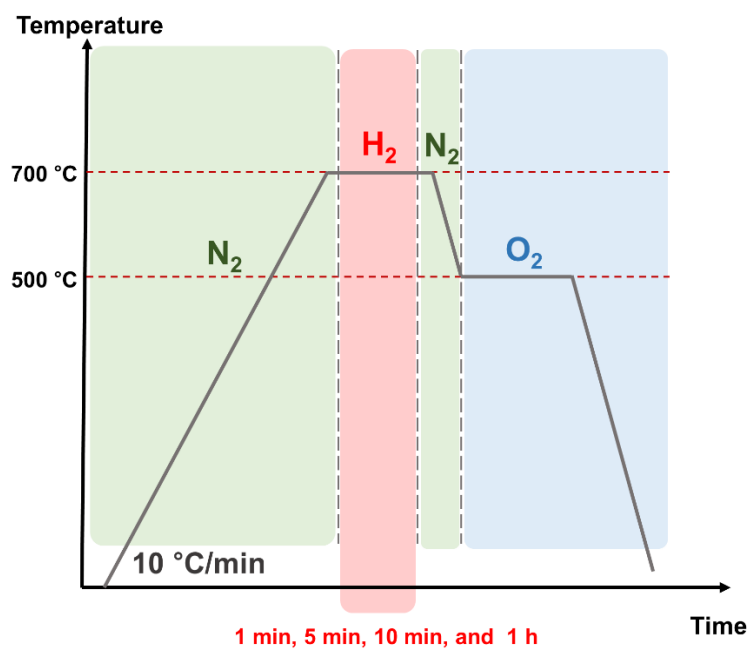
Table S3. Surface and bulk Pd/Al atomic ratio of various Pd-exchanged SSZ-13 samples prepared using different combinations of precursors, zeolite-forms, and calcination conditions.

Precursor species	Zeolite form	Ramping rate for calcination	Surface Pd/Al atomic ratio ^a		Bulk Pd/Al atomic ratio ^b
			Before calcination	After Calcination	
Pd(NH ₃) ₄ Cl ₂	NH ₄ -SSZ13	1 K/min		0.026	0.030
Pd(NH ₃) ₄ Cl ₂	NH ₄ -SSZ13		0.022	0.023	0.029
Pd(NH ₃) ₄ Cl ₂	H-SSZ13		0.025	0.022	0.029
Pd(NO ₃) ₂	NH ₄ -SSZ13	10 K/min	0.180	0.022	0.029
Pd(NO ₃) ₂	H-SSZ13		0.163	0.018	0.028

^a determined by XPS analysis.

^b determined by ICP-AES.

Supporting scheme



Scheme S1. Schematic description of the thermal treatment process.

Supporting movie captions

Movie S1. TEM movies and corresponding live FFT patterns of the ultramicrotomed Full-Pd²⁺/SSZ-13 (Si/Al=4.5), Pd/ZSM-5 (Si/Al=11.5), and NH₄-mordenite (Si/Al=10), operated under room temperature and with acceleration voltage of 200 kV. The radiolysis rate of different zeolites are monitored by the disappearance of peaks in FFT patterns. For Full-Pd²⁺/SSZ-13 samples, the peaks in live FFT patterns are fully unobservable after 10 s of electron-beam irradiation, whereas for Pd/ZSM-5 samples and NH₄-mordenite samples, the major peaks of live FFT patterns are still observable after 20 s of electron-beam irradiation. To directly compare the electron-beam-induced radiolysis of different zeolite samples, all samples are ultramicrotomed into ~50 nm thick sections and all TEM movies start from the initial stage of electron beam irradiation.

Movie S2. TEM movie of the ultramicrotomed thermal-treated Pd/SSZ-13 catalyst with 5 min of H₂ treatment, operated under room temperature and cryogenic temperature of -180 °C. The radiolysis of SSZ-13 was significantly reduced at cryogenic imaging mode.